Research Article

Hacettepe University Journal of the Faculty of Pharmacy
Volume 46 / Number 2 / June 2026 / pp. 137-148

Alginate–Basil Seed Hydrogel Films for Sustained Topical Delivery of Silver Sulfadiazine

Kailas Krishnat MALI[1]*
ORCID: 0000-0002-1789-3592
Vijay Daulatrao HAVALDAR[2]
ORCID: 0009-0006-7092-5609
Pratiksha Dadaso NARUTE[1]
ORCID: 0009-0001-7489-5551
Niranjan MAHAJAN[1]
ORCID: 0000-0002-2432-4507
Remeth Jacky DIAS[3]
ORCID: 0000-0002-8234-9630

[1]Department of Pharmaceutics, Adarsh College of Pharmacy, Vita, A/p - 421/2, Near MIDC, Khambale (Bha.), Vita, Tal- Khanapur 415311 Dist- Sangli, Maharashtra, India

[2]Department of Pharmacy, Adarsh Institute of Pharmacy, Bhavaninagar, Vita-Kindal Road, Vita, Tal- Khanapur 415311 Dist- Sangli, Maharashtra, India

[3]Department of Pharmacy, Government College of Pharmacy, Karad 415124 Dist- Satara, Maharashtra, India

Corresponding author:
Kailas Krishnat MALI
Department of Pharmaceutics
Adarsh College of Pharmacy,
Vita A/p - 421/2, Near MIDC, Khambale (Bha.), Vita Tal- Khanapur 415311
Dist- Sangli, Maharashtra, India
E-mail: malikailas@gmail.com
Tel: +91 9271546968,

Received date : 28.06.2025
Accepted date : 21.01.2026

DOI: 10.52794/hujpharm.1729518

ABSTRACT

This study developed and evaluated silver sulfadiazine (SSD)-loaded hydrogel films based on sodium alginate (SA) and basil seed mucilage (BSM) for controlled topical delivery. Films were formulated by varying SA (800–1000 mg) and BSM (50–200 mg) with calcium chloride ($CaCl_2$) (5–15%) as the crosslinker and propylene glycol (15% w/w) as a plasticizer. The optimized film (900 mg SA, 100 mg BSM, 10% $CaCl_2$, 30 min) was selected for its superior integrity and swelling. Attenuated Total Reflectance–Fourier Transform Infrared Spectroscopy (ATR–FTIR), Differential Scanning Calorimetry (DSC), Thermogravimetric Analysis (TGA), and X-ray Diffraction (XRD) confirmed SSD compatibility and uniform polymer dispersion. The optimized film exhibited high swelling (~38 g/g), moderate thickness (~609 µm), excellent flexibility (~252 folds), optimum tensile strength (0.454 kg/cm^2) and good surface wettability (~48° contact angle), reflecting balanced hydrophilicity and mechanical strength. In vitro release followed Fickian diffusion (Korsmeyer–Peppas $n < 0.45$), while additional evaluations confirmed appropriate water vapor transmission, microbial barrier properties, and hemocompatibility (< 5% hemolysis), supporting its biocompatibility. Overall, SA–BSM hydrogel films show strong potential as wound dressings, offering a stable, biocompatible matrix for sustained SSD delivery. However, as the study was limited to in vitro evaluations, further in vivo, stability, wound healing, and mechanical studies are warranted.

Keywords: Sodium alginate, Basil seed mucilage, Hydrogel films, Silver sulfadiazine, Topical delivery.

1. Introduction

Hydrogels are three-dimensional polymeric networks capable of absorbing and retaining large amounts of water or biological fluids [1]. These networks are typically formed through physical or chemical crosslinking, resulting in a colloidal system that is insoluble in water but exhibits excellent swelling behavior. Their high water content, flexibility, and biocompatibility make them promising candidates for biomedical and pharmaceutical applications, including wound dressings, drug delivery systems, and tissue engineering scaffolds [2].

Natural polymer-based hydrogels have attracted significant attention in recent years owing to their biodegradability, non-toxicity, and ability to mimic the extracellular matrix [3]. Among them, sodium alginate (SA), an anionic polysaccharide from brown algae, is widely used. SA undergoes ionic crosslinking with divalent cations like calcium (Ca^{2+}), forming the characteristic "egg-box" structure that enhances mechanical strength and gelation [4]. Its carboxylic groups confer pH sensitivity and enable gel formation under mild conditions [5]. However, pure alginate hydrogels are often brittle, mechanically weak, and degrade rapidly under physiological conditions [6]the use of polymers such as sodium alginate (NaAlg. To overcome these limitations, blending SA with other natural mucilaginous polymers has proven effective. Such combinations-like SA with guar gum or gelatin-have been shown to improve flexibility, mechanical integrity, and swelling properties of hydrogel films [7].

Basil seed mucilage (BSM), extracted from *Ocimum basilicum* seeds, is a natural hydrocolloid rich in heteropolysaccharides such as glucomannan and xylan. When hydrated, the seeds rapidly swell, releasing mucilage that forms a gelatinous layer with excellent thickening, stabilizing, and film-forming properties[8]. BSM's biocompatibility, gelling ability, viscosity, biodegradability, and water-retention capacity make it an attractive candidate for blending with alginate to enhance hydrogel performance, particularly in dermal and wound care applications [9]. Recent studies have demonstrated the potential of SA–BSM combinations in biomedical and pharmaceutical contexts. Yari et al. (2020) developed calcium alginate beads coated with BSM for metformin delivery, showing improved stability and pH-responsive behavior [10]. Sodium alginate (SA. Srikhao et al. (2022) created pH-sensitive hydrogel beads with SA, BSM, and magnetic nanoparticles, achieving enhanced swelling and sustained release [11]. These findings underscore the synergistic interaction between SA and BSM, supporting their use in hydrogel systems for biomedical and wound-healing applications.

To strengthen the hydrogel structure, calcium chloride ($CaCl_2$) is commonly used as an ionic crosslinker. By adjusting the concentration and exposure time of $CaCl_2$, the characteristics of the hydrogel films can be optimized for specific applications [12].

Silver sulfadiazine (SSD) is a widely used topical antimicrobial agent for treating burns and skin wounds. However, conventional formulations like creams and ointments are prone to removal or displacement, diminishing their effectiveness. Film-forming hydrogels address this limitation by adhering to the wound surface and enabling sustained drug release. SSD remains active in wound exudate, providing a favorable healing environment, and its broad-spectrum antimicrobial activity with prolonged site retention making it an excellent candidate for controlled topical delivery via hydrogel films [13]. Despite these advantages, limited research has investigated calcium chloride–crosslinked hydrogel films made from SA and BSM for SSD delivery. Most studies have focused on synthetic polymers or alginate alone, with little exploration of natural, synergistic blends like SA–BSM.

The present study aimed to formulate and evaluate silver sulfadiazine-loaded hydrogel films using SA and BSM, crosslinked with calcium chloride. The goal was to enhance matrix integrity, prolong drug release, and improve film flexibility for superior topical application. The study investigated the effects of polymer ratios and crosslinker concentration on swelling behavior, along with the films physicochemical and functional properties. This novel approach offers a promising, biocompatible drug delivery platform for burn and wound care.

2. Materials and Methods

2.1. Materials

Sodium alginate (medium viscosity, molecular weight ≈ 216,000 g/mol; viscosity 250-350 cps for 1% w/v solution at 25°C) was obtained from Research Lab

Fine Chem Industries, Mumbai, India. Basil seeds were procured from a local market and used for the extraction of mucilage (authenticated by Dr. Shankar M. Shendage, Department of Botany, Balwant College, Vita, Sangli-415311, identified as *Ocimum basilicum* L., family Lamiaceae). Silver sulfadiazine was purchased from Yarrow Chem Products Pvt. Ltd., Mumbai, India. All other chemicals and reagents used in the study were of analytical grade.

2.2. Extraction and purification of basil seed mucilage

Basil seeds (50 g) were soaked in distilled water for 2 h to swell, then homogenized at 500 rpm for 15 min to release mucilage. The mixture was filtered through muslin cloth, yielding ~500 mL mucilage. To this, 616 mL of 95% ethanol was added to precipitate the mucilage, which was collected with cotton cloth, washed with 30 mL acetone, air-dried (20 min), then oven-dried at 50 °C. For purification, the mucilage was mixed with three volumes of 95% ethanol, stored overnight at 4 °C, sieved, redispersed in water, and stirred for 30 min. The dispersion was dried in a vacuum oven at 50 °C, ground to a fine powder, and stored airtight for further use [14].

2.3. Preparation of SA-BSM hydrogel film

Hydrogel films were prepared using the solvent casting and ionic crosslinking method with varying ratios of SA and BSM. A 2% w/v polymer solution was prepared in distilled water and stirred at 1000 rpm for 2 h, followed by addition of 0.5 mL propylene glycol as plasticizer and further stirring for 10 min. The mixture was cast into petri dishes and left overnight to remove air bubbles, then dried at 50 °C for 24 h. Dried films were peeled and crosslinked in calcium chloride ($CaCl_2$) solution, washed with distilled water, dried again at 50 °C for 1 h, and stored in a desiccator. Preformulation studies were conducted using SA and BSM individually to determine optimal $CaCl_2$ concentration. Final formulations were optimized by adjusting $CaCl_2$ concentration and exposure time. Composition details are provided in Table 1.

2.4. Characterization of hydrogel film

Samples were characterised by Attenuated Total Reflectance–Fourier Transform Infrared Spectroscopy (ATR–FTIR), Differential Scanning Calorimetry (DSC), Thermogravimetric Analysis (TGA), and X-ray Diffraction (XRD) [15–17]. This investigation explored citric acid crosslinked hydroxyethyl tamarind gum hydrogel films as a potential biomaterial for drug delivery. Hydroxyethylation of tamarind gum aimed to improve its solubility, swelling, and crosslinking potential. The synthesized hydroxyethylated tamarind gum (HETG.

2.5. Practical yield

The practical yield of the hydrogel film was determined by comparing the final weight of the dried film to the initial total weight of the polymer and drug used [18]solid-state 13C-nuclear magnetic resonance (13C-NMR.

2.6. Thickness of hydrogel films

The thickness of hydrogel film was measured using a micrometer screw gauge [19].

Table 1. Composition of SA-BSM hydrogel films

Batch	A	B	C	D	E	F	G	H	I
Sodium alginate (mg)	1000	1000	1000	1000	1000	950	900	850	800
Basil seed mucilage (mg)	-	-	-	-	-	50	100	150	200
Propylene glycol	15%	15%	15%	15%	15%	15%	15%	15%	15%
After drying films were exposed to calcium chloride for crosslinking									
Calcium chloride	10%	10%	10%	5%	15%	10%	10%	10%	10%
Exposure time (min)	15	30	45	30	30	30	30	30	30

*Total polymer concentration is 2% w/v.

ISSN: 2458 - 8806

2.7. Folding endurance and tensile strength

Folding endurance of hydrogel film was determined as per reported procedure without any change [20]. Tensile strength of film was determined using a custom-built testing setup as reported earlier [16].

2.8. Wettability study

Hydrogel film wettability was assessed via water contact angle. A 10 µL distilled water droplet was placed on the film, imaged within 5 s, and analyzed using ImageJ software. Measurements were done in triplicate, and mean values reported [21]and Kollidon or microcrystalline cellulose was used as the disintegrant. Meloxicam (MLX.

2.9. Drug content

An accurately weighed 50 mg portion of the hydrogel film was soaked in 1 mL of 0.5% ammonia solution for 10 minutes, followed by dilution with phosphate buffer saline (PBS, pH 7.4) to a final volume of 20 mL. The mixture was stirred until complete dissolution, filtered, and analysed spectrophotometrically at 254 nm using a UV–Visible spectrophotometer (Shimadzu, Japan). Drug content was calculated using the standard calibration curve [22].

2.10. Swelling study

Swelling study of hydrogel film was performed as per reported method [23]. In brief, a pre-weighed hydrogel film (1 cm × 1 cm) was immersed in PBS (pH 7.4). At set intervals (30–1440 min), the film was removed, blotted, and reweighed.

2.11. Drug release

SSD release from hydrogel films was studied in PBS (pH 7.4). The release medium was maintained in a constant-temperature shaker (Remi, Ahmedabad) at 37 ± 0.5 °C with a shaking rate of 50 rpm. A 50 mg film was immersed in 40 mL PBS, and aliquots were withdrawn at set intervals, replaced with fresh PBS, filtered, and analysed at 254 nm. Experiments were performed in triplicate. Release data were fitted to zero-order, first-order, Higuchi, and Korsmeyer-Peppas models, and the best-fit model was determined from R^2 values [22].

2.12. Water vapour permeability test of hydrogel film

The water vapour transmission rate of hydrogel films was measured using the desiccant method. Glass vials (10 mL) containing anhydrous $CaCl_2$ were sealed with 2 cm-diameter films using Teflon tape, maintaining ~10 mm distance from the desiccant. A control vial without film was also prepared. Vials were kept in a desiccator with saturated NaCl solution (~75% RH) and weighed at 0, 6, 12, 24, 36, 48, and 72 h [15].

2.13. Microbial permeation test of hydrogel film

Hydrogel films' microbial barrier properties were evaluated using sterile 10 mL vials (2 cm diameter) containing 5 mL nutrient broth. Films were secured over the vial openings with Teflon tape. Positive (open vial) and negative (sealed with sterile cotton) controls were included. All vials were incubated at 37 °C for 7 days, and broth was monitored daily for turbidity indicating microbial contamination [24].

2.14. Hemocompatibility study

Hydrogel films (2 cm^2) were pre-swollen in PBS (pH 7.4) at 37 °C for 1 h. After removing PBS, 0.5 mL goat Citrate-Phosphate-Dextrose (CPD) blood was added, incubated for 20 min, and haemolysis was stopped with 4 mL of 0.9% NaCl. Samples were further incubated at 37 °C for 1 h and centrifuged at 4000 rpm for 10 min. Supernatant absorbance was measured at 545 nm (UV-1800, Shimadzu). Goat blood was obtained as waste from a slaughterhouse; no live animals were used. Hemocompatibility testing followed Mali et al., 2017 [25].

2.15. Statistical analysis

All quantitative results are expressed as mean ± SD. Statistical analysis was performed using one-way ANOVA followed by Tukey's post hoc test, and $p < 0.05$ was considered statistically significant.

3. Results and Discussion

3.1. Preparation of SA-BSM hydrogel film

The preformulation study optimized the SA–BSM ratios, $CaCl_2$ concentration, and exposure time for hydrogel film formation. Increasing BSM (0–200 mg) at

a fixed 2% w/v polymer concentration improved film flexibility and uniformity, with optimal properties at 50–100 mg [26]. $CaCl_2$ concentration (5–15%) and exposure time (15–45 min) influenced crosslinking. Films treated with 10% $CaCl_2$ for 30 min showed optimal integrity and flexibility, whereas lower concentrations lacked structure and higher ones were brittle [11]. Propylene glycol (15% w/w) was included as a plasticizer to reduce brittleness and improve handling [27]. The optimized formulation batch G (SA: 900 mg; BSM: 100 mg; $CaCl_2$: 10%; exposure: 30 min) exhibited desirable mechanical and swelling properties, confirming effective ionic crosslinking [28].

3.2. Mechanism of crosslink formation and scheme of synthesis

Sodium alginate and BSM are natural polysaccharides rich in hydroxyl (–OH) and carboxyl (–COOH) groups, enabling effective crosslinking. In this study, calcium chloride acted as an ionic crosslinker: Ca^{2+} ions interacted with the carboxylate groups of SA, forming stable junction zones via the well-known "egg-box" model and creating a robust 3D crosslinked network that reinforced film integrity [26]. BSM enhanced the matrix through intermolecular hydrogen bonding and chain entanglement, complementing ionic interactions and improving flexibility, elasticity, and homogeneity [29]. Crosslinking mechanism of hydrogel film is given in Figure 1.

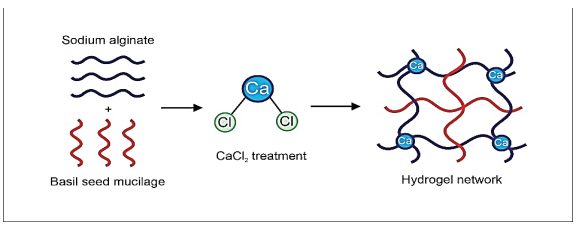

Figure 1. Crosslinking mechanism of hydrogel film

At the molecular level, Ca^{2+} ions preferentially bind to guluronic acid blocks in alginate, increasing cohesion, while the mucilaginous BSM ensured uniform dispersion and moisture retention. Propylene glycol further improved pliability and handling without disrupting crosslinking [30]cellouronic acid sodium (CAS. Together, $CaCl_2$ crosslinking, BSM's gelling properties, and propylene glycol's plasticizing effect yielded hydrogel films with superior strength, flexibility, and water absorption, suitable for topical and biomedical applications [31].

3.3. Characterization of hydrogel film

3.3.1. ATR-FTIR study

ATRFTIR (Figure 2) analyzed SA, BSM, SSD, and their hydrogel films (B and G batches). SA and BSM showed typical –OH, C–H, COO^-, and C–O–C peaks, indicating hydrophilic polysaccharide structures [32,33]hydrogels have been widely applied as draw agents in forward osmosis (FO. SSD displayed C–H, amide/C=N, and SO_2 stretches, confirming its aromatic and polar groups [34]. In B-loaded films, broad –OH stretching and alginate COO^- peaks suggested hydrogen bonding, while characteristic SSD peaks were absent, indicating molecular dispersion or interactions with the polymer [35]. G-loaded films (SA+BSM+SSD) showed intensified –OH and C–O–C bands and shifted COO^- peaks, reflecting stronger hydrogen bonding and cohesive network formation due to BSM incorporation, with SSD well embedded in the matrix [36].

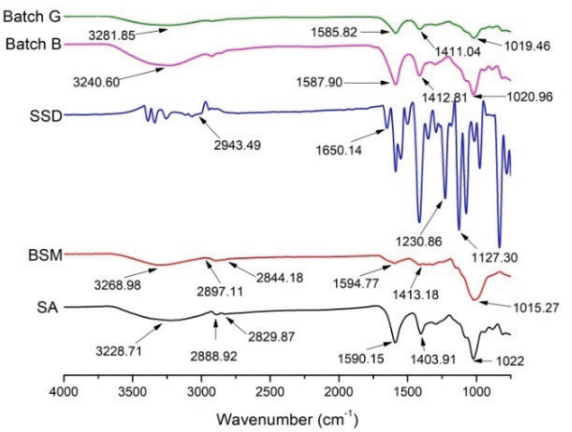

Figure 2. ATR-FTIR of SA, BSM, SSD, and Batch B, Batch G

3.3.2. Thermal analysis

DSC analysis (Figure 3A) evaluated thermal behavior and interactions of SA, BSM, SSD, and hydrogel films (B and G batches). SSD showed a sharp melting peak at ~285–290 °C, confirming high crystallinity and thermal stability [37]. SA and BSM exhibited moisture loss (~75–90 °C) and degradation peaks (~250–310 °C), indicating good thermal resistance [38]. In the B-loaded film (SA+SSD), peaks shifted slightly higher with reduced intensity, suggesting enhanced thermal stability and drug–polymer interac-

ISSN: 2458 - 8806

tions. The G-loaded film (SA+BSM+SSD) showed reduced and shifted degradation peaks, reflecting disrupted crystallinity and formation of a more amorphous, stable matrix. These changes confirm SSD molecular dispersion and improved thermal properties, particularly in the BSM-containing G batch [39].

TGA (Figure 3B) assessed thermal stability of SA, BSM, SSD, and hydrogel films (B and G batches). SSD was most stable, with minimal weight loss below ~275 °C and major degradation at 275–475 °C, leaving ~55% residue [9]. SA and BSM lost moisture below 150 °C and degraded between 225–350 °C, leaving ~30–35% residue, indicating suitability for processing up to ~200 °C. Drug-loaded films (B and G) showed slower, more gradual degradation than unloaded films, reflecting improved thermal stability via drug–polymer interactions and synergistic stabilization by BSM. Overall, SSD strengthened the polymer matrix, enhancing film resilience for wound dressing applications [40].

3.3.3. X-ray diffraction

XRD analysis (Figure 4) assessed the crystallinity of SA, BSM, SSD, and their formulations. Pure SSD showed sharp peaks (2θ ~7°, 12°, 17°), confirming its crystalline, stable structure [41]. The physical mixture (SA+BSM+SSD) retained some peaks below 30° 2θ, indicating partial SSD crystallinity. In the B-loaded film (SA+SSD), peak intensity decreased, reflecting reduced crystallinity and SSD dispersion in the amorphous SA matrix [42]. The G-loaded film (SA+BSM+SSD) exhibited a broad, diffuse pattern, suggesting near-complete loss of crystalline order due to interactions with SA and BSM. This progressive decrease in crystallinity enhances SSD's solubility, stability, and suitability for controlled topical delivery [38].

3.4. Practical yield

The practical yield of films ranged from 0.93 g (batch I) to 1.33 g (batch E). The highest yield in batch E, containing 15% $CaCl_2$, is attributed to enhanced ionic crosslinking, which reduced polymer dissolution during washing. In contrast, BSM-rich formulations (batches F–I) showed a progressive decline in yield (Table 2), likely due to BSM's lower ionic crosslinking capacity compared to alginate, resulting in weaker structural integrity and greater material loss during processing. [26].

3.5. Thickness of hydrogel films

Film thickness ranged from 518.66 µm (batch E) to 632.33 µm (batch I). Higher $CaCl_2$ concentration, as in batch E, produced denser networks and thinner films. In contrast, increasing BSM content (batches F–I) led to progressively thicker films (Table 2), likely due to BSM's water-retention capacity and its tendency to expand the gel structure despite crosslinking [43].

3.6. Folding endurance and tensile strength

The tensile strength (0.361–0.678 kg/cm²) and folding endurance (112–288 folds) of the hydrogel films are presented in Table 2. Increased $CaCl_2$ concentration (batch E) and longer exposure time (batch C) significantly increased tensile strength ($p < 0.05$) but decreased folding endurance ($p < 0.05$), likely due to

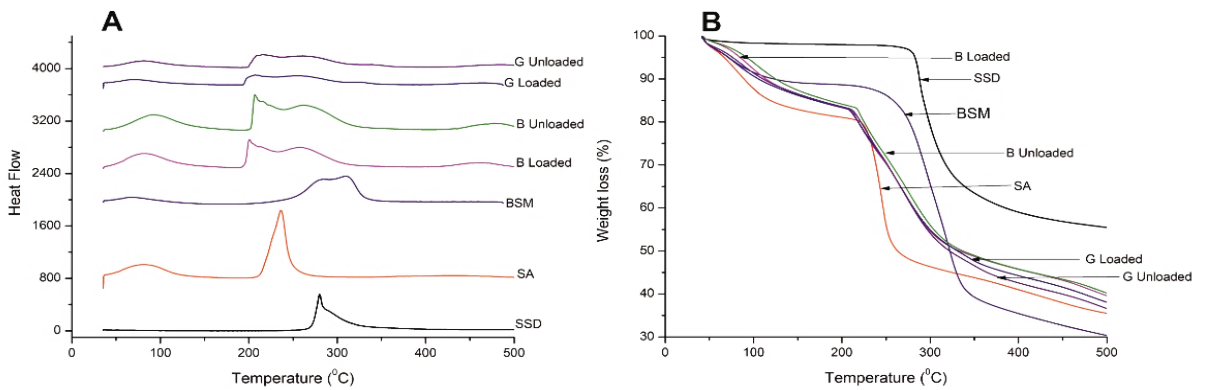

Figure 3. DSC (A) and TGA (B) of SSD, SA, BSM, Loaded and Unloaded B, G batches

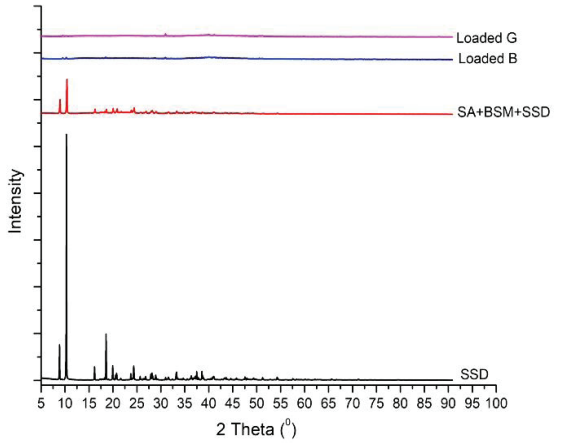

Figure 4. XRD of SA, BSM, SSD, Loaded B and G

formation of rigid, less flexible films. Incorporation of BSM (batches F–I) reduced tensile strength but improved folding endurance, attributed to BSM's flexible polymer chains enhancing film elasticity and resilience [44].

3.7. Wettability study

All hydrogel films exhibited hydrophilic behavior, with contact angles ranging from 36.74° to 54.73° (Table 2). Films with lower $CaCl_2$ levels (e.g., batch D) showed superior wettability, likely due to greater surface availability of hydrophilic groups. In contrast, higher BSM content increased contact angles, possibly from denser matrices and reduced surface accessibility [45]. Overall, formulations with 10% $CaCl_2$ and 50–100 mg BSM achieved an optimal balance of structural integrity and wettability, supporting their potential for biomedical and wound-healing applications.

3.8. Drug content

All the films exhibited drug content exceeding 90%, which confirms the uniform dispersion of silver sulfadiazine within the polymeric matrix [13].

3.9. Swelling study

The swelling behavior of hydrogel films was assessed in PBS (pH 7.4) to simulate physiological conditions. All formulations (A–I) showed an initial rapid swelling phase, reaching equilibrium within 6–8 hours (Figure 5A). Batch G (SA 900 mg + BSM 100 mg) exhibited the highest swelling (~38 g/g at 24 h), reflecting optimal hydrophilicity and matrix flexibility from its balanced polymer composition. In contrast, batch E (15% $CaCl_2$) had the lowest swelling (~28 g/g) due to its high crosslinking density restricting water uptake, while batch D (5% $CaCl_2$) showed rapid initial uptake but declined after 8 hours, likely from poor matrix stability. These results confirm that both $CaCl_2$ concentration and BSM content significantly influence hydration. Overall, batch G demonstrated an optimal swelling profile, making it well-suited for wound dressing and controlled drug release applications [46].

Table 2. Evaluation of SA-BSM hydrogel films

Batch	Practical Yield (g)	Thickness (μm)	Folding Endurance	Tensile strength (kg/cm²)	**Contact Angle (°)**	**WVTR (g/m²)**	Haemolysis (%)
A	1.09±0.01	612.77±11.57	217±46.13	0.483±0.002	40.81±0.19	975.50	3.93
B	1.22±0.10	598.89±9.25	137.67±23.79	0.565±0.003	38.72±3.12	909.02	2.01
C	1.26±0.02	587.77±9.56	117.67±12.83	0.622±0.003	41.55±1.90	898.09	2.33
D	1.04±0.01	620.55±18.57	288±4.96	0.361±0.001	36.74±2.62	977.16	3.03
E	1.33±0.04	518.66±7.20	112±41.78	0.678±0.003	41.37±2.39	843.01	2.77
F	1.00±0.03	605.22±3.96	177.33±51.79	0.510±0.002	40.11±2.27	1108.13	4.02
G	0.98±0.04	609.69±1.91	252.33±41.78	0.454±0.002	48.82±2.54	1148.74	3.00
H	0.95±0.06	622.05±1.59	255.67±17.74	0.413±0.002	42.54±1.83	1281.58	2.47
I	0.93±0.01	632.33±1.20	283.33±38.31	0.395±0.001	54.73±1.74	1289.95	4.72

*Readings are expressed as Average ± Standard Deviation of triplicate samples; WVTR: water vapour transmission rate.

ISSN: 2458 - 8806

3.10. Drug release

The cumulative drug release profile of silver sulfadiazine (SSD) from the hydrogel films (Figure 5B) showed a biphasic pattern: an initial burst followed by sustained release, typical of hydrophilic polymer matrices. Among all batches, batch G achieved the highest and most controlled release (~92.8% over 6 hours), attributed to its optimized SA (900 mg) and BSM (100 mg) composition, which provided a balanced matrix with adequate hydration and porosity. Moderate crosslinking (10% $CaCl_2$, 30 min) maintained structural integrity while permitting water penetration and drug diffusion. In contrast, batch D (5% $CaCl_2$) released ~91% faster due to a weaker, more porous matrix, whereas batch E (15% $CaCl_2$) showed the lowest release (~76%) due to dense crosslinking that limited water uptake and drug mobility. Kinetic analysis (Table 3) indicated the Korsmeyer–Peppas model best described batch G's release ($R^2 = 0.962$) with a release exponent n = 0.29, confirming Fickian diffusion as the dominant mechanism. These findings demonstrate that batch G offers an optimal balance of hydration, stability, and sustained SSD release, making it a promising candidate for topical drug delivery [37].

To elucidate the mechanism of SSD release, the drug release data for all batches were fitted to various kinetic models, including Zero-order, Higuchi, and Korsmeyer–Peppas. The Korsmeyer–Peppas model showed the best fit for most formulations, as indicated by the highest correlation coefficients (R^2), suggesting that release is primarily diffusion-controlled through the hydrated polymer network. The release exponent (n) values were below 0.5 for all batches, confirming Fickian diffusion as the dominant mechanism, where drug release occurs mainly via diffusion rather than matrix swelling or erosion. The low n values reflect the crosslinked hydrogel structure, formed by ionic interactions with $CaCl_2$, which limits polymer relaxation and water uptake, resulting in a controlled release profile. The consistently high R^2 values for the Korsmeyer–Peppas model across all batches reinforce diffusion as the main release mechanism. Overall, the data demonstrate that the hydrogel films provide a sustained, diffusion-driven release of SSD, making them promising for topical drug delivery. Detailed kinetic parameters (n, R^2, and best-fit models) are presented in Table 3.

3.11. Water vapour permeability test of hydrogel film

Water vapour transmission rate (WVTR) is crucial for wound dressings to maintain optimal moisture. The prepared films exhibited WVTR values between 975.50 and 1289.95 g/m²/24 h (Table 2), compared to 1898.78 g/m²/24 h for the control, which was more permeable. SA-only films (batches A–E) showed lower WVTR due to dense $CaCl_2$ crosslinking, with batch E (15% $CaCl_2$) having the lowest, indicating a compact structure. In contrast, BSM-containing films (batches F–I) displayed higher WVTR, attributed to the hydrophilic and porous nature of BSM. Batch I

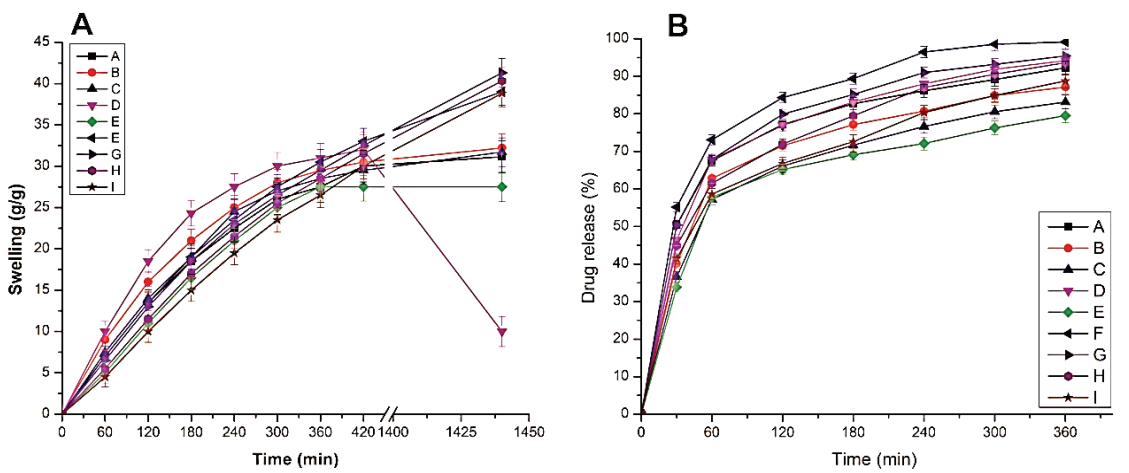

Figure 5. Swelling study (A) and drug release (B) of hydrogel films in phosphate buffer saline pH 7.4

(200 mg BSM) had the highest WVTR, suggesting enhanced moisture permeability. Overall, increasing BSM improved vapour transmission, supporting the films' suitability for wound healing [47].

3.12. Microbial permeation test of hydrogel film

The microbial barrier function of SA–BSM hydrogel films was evaluated over 7 days. No microbial growth was detected in any hydrogel-containing vials (batches A–I) throughout the study, whereas control vials became turbid by day 4, with increased turbidity by day 7. These findings demonstrate that the hydrogel films effectively prevent microbial penetration, supporting their potential application in wound care [48]thermo-stability, sol-gel transformation and drug release.

3.13. Hemocompatibility study

A haemolysis study was performed to assess the hemocompatibility of hydrogel films (batches A–I). As shown in Table 2, all films exhibited haemolysis percentages below the critical 5% threshold, confirming their suitability for blood-contact applications. Minor variations between batches likely reflect differences in surface properties or residual crosslinkers, but all remained within the safe range, supporting their potential for biomedical use [49].

4. Conclusion

The formulated SA-BSM hydrogel films incorporating silver sulfadiazine demonstrated promising characteristics for topical drug delivery applications. The optimized formulation (batch G) exhibited enhanced swelling capacity, controlled drug release following Korsmeyer-Peppas with Fickian diffusion, desirable water vapor transmission, and acceptable hemocompatibility. ATR-FTIR, DSC, TGA, and XRD analyses confirmed strong intermolecular interactions and successful drug incorporation within a stable polymeric matrix. Overall, SA–BSM hydrogel films represent a stable, biocompatible, and multifunctional platform for sustained SSD delivery and wound healing applications. Despite encouraging results, the study was limited to in vitro evaluations. Future work should assess in vivo biocompatibility, wound healing, and mechanical properties.

Acknowledgement

The authors are thankful to Adv. Vaibhav (Dada) Patil, President of the Loknete Hon. Hanmantrao Patil Charitable Trust, Vita, for providing the necessary facilities to carry out the research work. Shivaji University, Kolhapur; Krishna Vishwa Vidyapeeth, Karad; and Sadguru Gadage Maharaj College, Karad are acknowledged for their assistance with analytical work.

Table 3. Drug release kinetics of hydrogel films

Batch	Korsmeyer-Peppas release exponent (n)	Korsmeyer-Peppas R^2	Zero order R^2	Higuchi R^2	Release mechanism
A	0.27	0.953	0.828	0.920	Fickian diffusion
B	0.35	0.901	0.790	0.886	Fickian diffusion
C	0.36	0.914	0.827	0.915	Fickian diffusion
D	0.32	0.922	0.820	0.911	Fickian diffusion
E	0.38	0.860	0.760	0.856	Fickian diffusion
F	0.27	0.955	0.820	0.916	Fickian diffusion
G	0.29	0.962	0.829	0.923	Fickian diffusion
H	0.31	0.969	0.893	0.964	Fickian diffusion
I	0.30	0.940	0.905	0.965	Fickian diffusion

ISSN: 2458 - 8806

Conflict of Interest

The authors declare that they have no conflict of interests.

Statement of Contribution of Researchers

Concept, Design, Resources, Materials, Writing – K.K.M., P.D.N; Supervision – K.K.M., N.S.M,; Data Collection and/or Processing– K.K.M., V.D.H., N.S.M.; Analysis and/or Interpretation –R.J.D., V.D.H., N.S.M.; Literature Search– P.D.N; Critical Reviews- R.J.D., V.D.H.

References

1. Mozaffari E, Tanhaei B, Khajenoori M, Movaghar Khoshkho S. Unveiling the swelling behavior of κ-carrageenan hydrogels: Influence of composition and physiological environment on drug delivery potential. J Ind Eng Chem. 2025; 141: 217–27. https://doi.org/10.1016/j.jiec.2024.06.032.
2. Sharmin N, Sone I, Walsh JL, Sivertsvik M, Fernández EN. Effect of citric acid and plasma activated water on the functional properties of sodium alginate for potential food packaging applications. Food Packag Shelf Life. 2021; 29: 100733. https://doi.org/10.1016/j.fpsl.2021.100733.
3. He C, Bi S, Zhang L, Gu J, Yan B. An antioxidative sodium alginate hybrid hydrogel with NIR-controlled NO releasing for diabetic wound healing via reduced inflammation and enhanced angiogenesis. Carbohydr Polym. 2025; 366: 123913. https://doi.org/10.1016/j.carbpol.2025.123913.
4. Kapoor DU, Pareek A, Sharma S, Prajapati BG, Thanawuth K, Sriamornsak P. Alginate gels: Chemistry, gelation mechanisms, and therapeutic applications with a focus on GERD treatment. Int J Pharm. 2025; 675: 125570. https://doi.org/10.1016/j.ijpharm.2025.125570.
5. Wang H, Liu J, Fan X, Ren J, Liu Q, Kong B. Fabrication, characterisation, and application of green crosslinked sodium alginate hydrogel films by natural crab-shell powders to achieve drug sustained release. LWT 2022; 171: 114147. https://doi.org/10.1016/j.lwt.2022.114147.
6. Bustos-Terrones YA. A Review of the Strategic Use of Sodium Alginate Polymer in the Immobilization of Microorganisms for Water Recycling. Polymers (Basel). 2024; 16: 788. https://doi.org/10.3390/polym16060788.
7. Shah Bukhary SKH, Choudhary FK, Iqbal DN, Ali Z, Sadiqa A, Latif S, et al. Development and characterization of a biodegradable film based on guar gum-gelatin sodium alginate for a sustainable environment. RSC Adv. 2024; 14: 19349–61. https://doi.org/10.1039/D4RA03985H.
8. Phonrat A, Subyai N, Prachayawarakorn J. Alternative Polysaccharide Wound Dressing from Heat-Moisture Starch/Basil Seed (O. Basilicum L.) Mucilage with Incorporated Glycolic Acid Antimicrobial Agent. J Macromol Sci Part B. 2025; 64: 845–66. https://doi.org/10.1080/00222348.2024.2367340.
9. Ullah S, Hashmi M, Kharaghani D, Khan MQ, Saito Y, Yamamoto T, et al. Antibacterial properties of in situ and surface functionalized impregnation of silver sulfadiazine in polyacrylonitrile nanofiber mats. Int J Nanomedicine. 2019; 14: 2693–703. https://doi.org/10.2147/IJN.S197665.
10. Yari K, Akbari I, Yazdi SAV. Development and evaluation of sodium alginate-basil seeds mucilage beads as a suitable carrier for controlled release of metformin. Int J Biol Macromol. 2020; 159: 1–10. https://doi.org/10.1016/j.ijbiomac.2020.04.111.
11. Srikhao N, Chirochrapas K, Kwansanei N, Kasemsiri P, Ounkaew A, Okhawilai M, et al. Multi-Responsive Optimization of Novel pH-Sensitive Hydrogel Beads Based on Basil Seed Mucilage, Alginate, and Magnetic Particles. Gels. 2022; 8: 274. https://doi.org/10.3390/gels8050274.
12. Su C, Li D, Wang L. From micropores to mechanical strength: Fabrication and characterization of edible corn starch-sodium alginate double network hydrogels with Ca2+ cross-linking. Food Chem. 2025; 467: 142276. https://doi.org/10.1016/j.foodchem.2024.142276.
13. Saranya T, Manoj K. Formulation, evaluation and optimization of novel silver sulfadiazine loaded film forming hydrogel for burns. Hygeia J Drugs Med 2016; 8: 1–10. https://doi.org/10.15254/H.J.D.Med.8.2016.156.
14. Guan L, Ma Y, Yu F, Jiang X, Jiang P, Zhang Y, et al. The recent progress in the research of extraction and functional applications of basil seed gum. Heliyon. 2023; 9: e19302. https://doi.org/10.1016/j.heliyon.2023.e19302.
15. Salunkhe NH, Mali KK, Sidwadkar PH, Pareek KM, Aundhakar AS. Synthesis and characterization of citric acid crosslinked garden cress seeds mucilage hydrogel for controlled drug release. J Drug Deliv Sci Technol. 2025;112:107270. https://doi.org/10.1016/j.jddst.2025.107270.
16. Ghorpade VS, Mali KK, Dias RJ, Dhawale SC, Digole RR, Gandhi JM, et al. Citric acid crosslinked hydroxyethyl tamarind gum-based hydrogel films: A promising biomaterial for drug delivery. Int J Biol Macromol. 2024; 282: 137127. https://doi.org/10.1016/j.ijbiomac.2024.137127.
17. Pargaonkar SS, Ghorpade VS, Mali KK, Dias RJ, Havaldar VD, Kadam VJ. Hydrogel Films of Citric Acid Cross-linked Hydroxypropyl Methylcellulose/Methylcellulose for Hydrophilic Drug Delivery. Indian J Pharm Educ Res. 2023; 57: 718–27. https://doi.org/10.5530/ijper.57.3.87.

18. Mali KK, Dhawale SC, Dias RJ, Ghorpade VS, Dhane NS. Development of vancomycin-loaded polysaccharide-based hydrogel wound dressings: In vitro and in Vivo evaluation. Asian J Pharm. 2018; 12: 94–105.

19. Lan W, He L, Liu Y. Preparation and Properties of Sodium Carboxymethyl Cellulose/Sodium Alginate/Chitosan Composite Film. Coatings. 2018; 8: 291. https://doi.org/10.3390/coatings8080291.

20. Singh B, Sharma S, Dhiman A. Design of antibiotic containing hydrogel wound dressings: Biomedical properties and histological study of wound healing. Int J Pharm. 2013; 457: 82–91. https://doi.org/10.1016/j.ijpharm.2013.09.028.

21. Jadach B, Misek M, Ferlak J. Comparison of Hydroxypropyl Methylcellulose and Alginate Gel Films with Meloxicam as Fast Orodispersible Drug Delivery. Gels. 2023; 9: 687. https://doi.org/10.3390/gels9090687.

22. Mastiholimath VS, Valerie CTW, Mannur VS, Dandagi PM, Gadad AP, Khanal P. Formulation and evaluation of solid lipid nanoparticle containing silver sulfadiazine for second and third degree burn wounds and its suitable analytical method development and validation. Indian J Pharm Educ Res. 2020; 54: 31–45. https://doi.org/10.5530/ijper.54.1.5.

23. Giz AS, Berberoglu M, Bener S, Aydelik-Ayazoglu S, Bayraktar H, Alaca BE, et al. A detailed investigation of the effect of calcium crosslinking and glycerol plasticizing on the physical properties of alginate films. Int J Biol Macromol. 2020; 148: 49–55. https://doi.org/10.1016/j.ijbiomac.2020.01.103.

24. Shao W, Liu H, Liu X, Wang S, Wu J, Zhang R, et al. Development of silver sulfadiazine loaded bacterial cellulose/sodium alginate composite films with enhanced antibacterial property. Carbohydr Polym. 2015; 132: 351–8. https://doi.org/10.1016/j.carbpol.2015.06.057.

25. Mali KK, Dhawale SC, Dias RJ. Synthesis and characterization of hydrogel films of carboxymethyl tamarind gum using citric acid. Int J Biol Macromol. 2017; 105: 463–70. https://doi.org/10.1016/j.ijbiomac.2017.07.058.

26. Hosseini MS, Nabid MR. Synthesis of chemically cross-linked hydrogel films based on basil seed (Ocimum basilicum L.) mucilage for wound dressing drug delivery applications. Int J Biol Macromol. 2020; 163: 336–47. https://doi.org/10.1016/j.ijbiomac.2020.06.252.

27. Janik W, Nowotarski M, Ledniowska K, Shyntum DY, Krukiewicz K, Turczyn R, et al. Modulation of physicochemical properties and antimicrobial activity of sodium alginate films through the use of chestnut extract and plasticizers. Sci Rep. 2023; 13: 11530. https://doi.org/10.1038/s41598-023-38794-3.

28. Arafa EG, Gawad OFA, Eldin ZE, Ibrahim MM, Abd-Elghafour SA, Osman AHM. Sustainable sodium alginate hydrogels incorporating banana leaf activated carbon and organo-clay for enhanced dye removal. Sci Rep. 2025; 15: 16197. https://doi.org/10.1038/s41598-025-99343-8.

29. Alam MN, Christopher LP. A novel, cost-effective and eco-friendly method for preparation of textile fibers from cellulosic pulps. Carbohydr Polym, 2017; 173: 253–8. https://doi.org/10.1016/j.carbpol.2017.06.005.

30. Zhang H, Gao X, Chen K, Li H, Peng L. Thermo-sensitive and swelling properties of cellouronic acid sodium/poly (acrylamide-co-diallyldimethylammonium chloride) semi-IPN. Carbohydr Polym. 2018; 181: 450–9. https://doi.org/10.1016/j.carbpol.2017.10.093.

31. Peter Z. Order in cellulosics: Historical review of crystal structure research on cellulose. Carbohydr Polym. 2021; 254: 117417. https://doi.org/10.1016/j.carbpol.2020.117417.

32. Saad MA, Sadik ER, Eldakiky BM, Moustafa H, Fadl E, He Z, et al. Synthesis and characterization of an innovative sodium alginate/polyvinyl alcohol bioartificial hydrogel for forward-osmosis desalination. Sci Rep. 2024; 14: 8225. https://doi.org/10.1038/s41598-024-58533-6.

33. Samiee Paghaleh E, Kolvari E, Seidi F, Dashtian K. Eco-friendly and sustainable basil seed hydrogel-loaded copper hydroxide-based catalyst for the synthesis of propargylamines and tetrazoles. Nanoscale Adv. 2024; 6: 960–72. https://doi.org/10.1039/D3NA01085F.

34. Bult A, Plug CM. Silver Sulfadiazine. Anal. Profiles Drug Subst. Excipients, vol. 13, 1984, p. 553–71. https://doi.org/10.1016/S0099-5428(08)60202-6.

35. Hashemi Gahruie H, Eskandari MH, Sadeghi R, Hosseini SMH. Atmospheric Pressure Cold Plasma Modification of Basil Seed Gum for Fabrication of Edible Film Incorporated with Nanophytosomes of Vitamin D3 and Tannic Acid. Foods. 2022; 12: 71. https://doi.org/10.3390/foods12010071.

36. Aswathy SH, NarendraKumar U, Manjubala I. Physicochemical Properties of Cellulose-Based Hydrogel for Biomedical Applications. Polymers (Basel). 2022; 14: 4669. https://doi.org/10.3390/polym14214669.

37. Kumar A, Pathak M. Formulation, Evaluation & in - Vivo Study of Topical Emul Gel Loaded With Silver Sulfadiazine for Wound. African J Biol Sci. 2024; 6: 3321–47. https://doi.org/10.33472/AFJBS.6.9.2024.3320-3366.

38. Ghumman SA, Noreen S, Hameed H, Elsherif MA, Shabbir R, Rana M, et al. Synthesis of pH-Sensitive Cross-Linked Basil Seed Gum/Acrylic Acid Hydrogels by Free Radical Copolymerization Technique for Sustained Delivery of Captopril. Gels. 2022; 8: 291. https://doi.org/10.3390/gels8050291.

ISSN: 2458 - 8806

39. Pereira R, Carvalho A, Vaz DC, Gil MH, Mendes A, Bártolo P. Development of novel alginate based hydrogel films for wound healing applications. Int J Biol Macromol. 2013; 52: 221–30. https://doi.org/10.1016/j.ijbiomac.2012.09.031.

40. Kalam MA. The potential application of hyaluronic acid coated chitosan nanoparticles in ocular delivery of dexamethasone. Int J Biol Macromol. 2016; 89: 559–68. https://doi.org/10.1016/j.ijbiomac.2016.05.016.

41. Dong Z, Wang Q, Du Y. Alginate/gelatin blend films and their properties for drug controlled release. J Memb Sci. 2006; 280: 37–44. https://doi.org/10.1016/j.memsci.2006.01.002.

42. Chalitangkoon J, Wongkittisin M, Monvisade P. Silver loaded hydroxyethylacryl chitosan/sodium alginate hydrogel films for controlled drug release wound dressings. Int J Biol Macromol. 2020; 159: 194–203. https://doi.org/10.1016/j.ijbiomac.2020.05.061.

43. Rezvanian M, Ahmad N, Cairul M, Mohd I, Ng S. International Journal of Biological Macromolecules Optimization, characterization, and in vitro assessment of alginate-pectin ionic cross-linked hydrogel film for wound dressing applications. Int J Biol Macromol. 2017; 97: 131–40. https://doi.org/10.1016/j.ijbiomac.2016.12.079.

44. Park SY, Kim W-J, Choi JB, Kim S. Physical and mechanical properties of alginate-based hydrogel film as carrier for release of acetylthiocholine. Int J Precis Eng Manuf 2018; 19: 129–35. https://doi.org/10.1007/s12541-018-0015-1.

45 Li X, Al-Assaf S, Fang Y, Phillips GO. Competitive adsorption between sugar beet pectin (SBP) and hydroxypropyl methylcellulose (HPMC) at the oil/water interface. Carbohydr Polym. 2013; 91: 573–80. https://doi.org/10.1016/j.carbpol.2012.08.075.

46. bt Ibrahim SF, Mohd Azam NAN, Mat Amin KA. Sodium alginate film: the effect of crosslinker on physical and mechanical properties. IOP Conf Ser Mater Sci Eng. 2019; 509: 012063. https://doi.org/10.1088/1757-899X/509/1/012063.

47. Tantiwatcharothai S, Prachayawarakorn J. Characterization of an antibacterial wound dressing from basil seed (Ocimum basilicum L.) mucilage-ZnO nanocomposite. Int J Biol Macromol. 2019; 135: 133–40. https://doi.org/10.1016/j.ijbiomac.2019.05.118.

48. Goh CH, Heng PWS, Chan LW. Alginates as a useful natural polymer for microencapsulation and therapeutic applications. Carbohydr Polym. 2012; 88: 1–12. https://doi.org/10.1016/j.carbpol.2011.11.012.

49. Mali KK, Havaldar VD, Salunkhe NH, Varude OS, Mahajan NS, Dias RJ. Development of carboxymethyl tamarind gum-based composite hydrogel films for wound dressing applications. Eur Pharm J. 2025; 6786:1–14. https://doi.org/10.2478/afpuc-2025-0010.